AGU100 ADVANCING EARTH AND SPACE SCIENCE

JGR

Journal of Geophysical Research: Atmospheres

RESEARCH ARTICLE
10.1002/2017JD027829

**Key Points:**
- Precipitation delta $^{18}O$ values in events mainly exhibit a V shape; reevaporation can affect delta $^{18}O$ values, specifically in the stratiform zone
- Convection activities in upwind area contribute more to variations in delta $^{18}O$ values of daily precipitation relative to on-site convection
- El Nino likely controls the regional organized convection in the area and thus affects the delta $^{18}O$ values of precipitation

**Supporting Information:**
- Supporting Information S1

**Correspondence to:**
S. He,
snhe@ntu.edu.sg

**Citation:**
He, S., Goodkin, N. F., Kurita, N., Wang, X., & Rubin, C. M. (2018). Stable isotopes of precipitation during tropical Sumatra Squalls in Singapore. *Journal of Geophysical Research: Atmospheres*, *123*, 3812–3829. https://doi.org/10.1002/2017JD027829

Received 30 SEP 2017
Accepted 11 MAR 2018
Accepted article online 14 MAR 2018
Published online 13 APR 2018



# Stable Isotopes of Precipitation During Tropical Sumatra Squalls in Singapore

**Shaoneng He[1], Nathalie F. Goodkin[1,2], Naoyuki Kurita[3], Xianfeng Wang[1,2], and Charles Martin Rubin[1,2]**

[1]Earth Observatory of Singapore, Nanyang Technological University, Singapore, [2]Asian School of the Environment, Nanyang Technological University, Singapore, [3]Graduate School of Environmental Studies, Nagoya University, Nagoya, Japan

**Abstract** Sumatra Squalls, organized bands of thunderstorms, are the dominant mesoscale convective systems during the intermonsoon and southwest monsoon seasons in Singapore. To understand how they affect precipitation isotopes, we monitored the $\delta$ value of precipitation daily and continuously (every second and integrated over 30 s) during all squalls in 2015. We found that precipitation $\delta^{18}O$ values mainly exhibit a "V"-shape pattern and less commonly a "W"-shape pattern. Variation in $\delta^{18}O$ values during a single event is about 1 to 6‰ with the lowest values mostly observed in the stratiform zone, which agrees with previous observations and modeling simulations. Reevaporation can significantly affect $\delta$ values, especially in the last stage of the stratiform zone. Daily precipitation is characterized by periodic negative shifts in $\delta$ value, largely associated with the squalls rather than moisture source change. The shifts can be more than 10‰, larger than intraevent variation. Initial $\delta^{18}O$ values of events are highly variable, and those with the lowest values also have the lowest initial values. Therefore, past convective activities in the upwind area can significantly affect the $\delta^{18}O$, and convection at the sampling site has limited contribution to isotopic variability. A significant correlation between precipitation $\delta^{18}O$ value and regional outgoing longwave radiation and rainfall in the Asian monsoon region and western Pacific suggests that regional organized convection probably drives stable isotopic compositions of precipitation. A drop in the frequency of the squalls in 2015 is related to weak organized convection in the region caused by El Niño.

## 1. Introduction

Oxygen and hydrogen isotopes of water are widely used as natural tracers of hydrological processes and past climate because light and heavy isotopes in water molecules are fractionated with variations in physical conditions during phase changes. A positive correlation between stable isotopes of precipitation and temperature, that is, the temperature effect, has long been used to interpret paleoclimate archives at high latitudes (Bowen, 2008; Dansgaard et al., 1993; Jouzel, 2003). At low latitudes in tropical regions, there is no consensus about the drivers of stable isotopes in precipitation (Bony et al., 2008; Kurita et al., 2009; Risi, Bony, & Vimeux, 2008). A negative correlation between rain amount and precipitation stable isotope compositions has been observed but only at monthly or long-term scales (Dansgaard, 1964; Kurita et al., 2009; Rozanski et al., 1993). Moreover, the amount affect is not universal, varying across the tropics (e.g., Aggarwal et al., 2004). Large variations in the stable isotope compositions of daily precipitation, up to more than 20 ‰, have been observed in the tropics, resulting from regional organized convection (He et al., 2014, 2015; Moerman et al., 2013; Permana et al., 2016; Sánchez-Murillo et al., 2016). In the tropics, most precipitation apparently arises from convective clouds (Houze, 1997). Tropical convective systems range from isolated to well-organized convective systems and from shallow to deep convective systems (Houze, 2004; Masunaga et al., 2005; Masunaga & Kummerow, 2006), and they are expected to have different degree of influence on stable isotopic composition of precipitation. Modeling studies suggest that cloud dynamics and physical processes associated with convection, including reevaporation, diffusive exchanges, and the recycling of depleted vapor from convective downdraft at the boundary layer, are the likely dominant drivers of stable isotope composition of precipitation (Bony et al., 2008; Kurita, 2013; Lee & Fung, 2008; Risi et al., 2010; Risi, Bony, & Vimeux, 2008; Tremoy et al., 2014). Several recent studies have shown that high temporal analysis of stable isotopes of precipitation during events reveal the relationship between the local and microphysical processes and the evolution in stable isotopic composition of precipitation (e.g., Barras & Simmonds, 2009; Muller et al., 2015; Rao et al., 2008; Risi et al., 2010). Advances in analytical technology, such as the invention of diffusion sampler (DS) (Munksgaard et al., 2012, 2011) and standard delivery module (Bonne et al., 2014; Tremoy et al., 2014), make it possible to continuously monitor the stable isotopic compositions of precipitation and vapor at high temporal resolution and allow us to observe the real-time evolution of stable isotopes of both precipitation and vapor.

Sumatra Squalls, narrow bands of thunderstorms, are the dominant organized convective systems in Singapore and the surrounding area during the intermonsoon (April–May and October–November) and southwest (SW) monsoon seasons (June–September, JJAS) with average frequencies of six to eight occurrences per month (Lo & Orton, 2016). The squalls generally form in Sumatra or along the Malacca Straits and move eastward over the Malay Peninsula and Singapore normally before dawn or in the early morning between April and November each year. They are usually hundreds of kilometers in length lasting several hours with gusty winds and heavy rains, impacting large areas in the region, including Sumatra, the Malay Peninsula, and Singapore (Yi & Lim, 2007). Understanding how convection during the squalls affects stable isotopes of precipitation will help us understand the drivers of variations in precipitation stable isotopes in the study area, ultimately improving interpretation of paleoclimate records in tropical regions.

In this study, we monitored all the Sumatra Squalls that made landfall in Singapore between April and October in 2015. Stable isotopic composition of precipitation was continuously analyzed during these squalls using a DS. Daily precipitation samples collected in 2014 and 2015 were also analyzed for stable isotope compositions, but in this study we only focused on the samples from the time periods related to Sumatra Squalls, and discussion of stable isotopes of daily precipitation over longer periods will be included in future studies. We utilized these data collected in this study to investigate the evolution of the stable isotopes in precipitation during the squalls, to understand how intraevent-scale isotopic variation is associated with convective cloud dynamics and physical processes during the squalls, and to evaluate the contribution of the squalls to the variation in stable isotopes of daily precipitation. One of the strongest El Niño events in recorded history evolved in 2015, affording the opportunity to examine El Niño impacts on the squalls and the stable isotopes of related precipitation. Our knowledge of the physical processes and their impact on stable isotopes during tropical convection is largely obtained from modeling studies (Bony et al., 2008; Kurita, 2013; Lee & Fung, 2008; Risi, Bony, & Vimeux, 2008; Risi et al., 2010; Tremoy et al., 2014). The high temporal resolution data collected in this study can also provide some insight into cloud dynamics during tropical convection and help to improve the related isotope-enabled models.

## 2. Data and Methods

### 2.1. Site Description

Our rain station was installed outside the Geochemistry Laboratories of the Asian School of the Environment (ASE) (1.35°N, 103.68°E, altitude 40 m above sea level) at Nanyang Technological University at the western edge of Singapore. This site is in the closest proximity to Sumatra and the Malacca Strait (Figure 1). Located just north of the equator, Singapore has a typical tropical climate with abundant rainfall, high and uniform temperature, and high humidity all year round. Its climate is mainly governed by the northeast (NE) and SW monsoons. The NE monsoon is accompanied by more frequent rain, particularly from December to January. The SW monsoon produces a marginally dryer climate from May to September, during which the climate is characterized by early-morning storms, normally organized into long lines extending for hundreds of kilometers, known as Sumatra squalls. The Squalls move towards Singapore from the west and eventually dissipate over the South China Sea (SCS).

### 2.2. Stable Isotope Analysis of Precipitation

A DS coupled to a Picarro L2130-*i*, an infrared spectroscopy instrument based on cavity ring-down spectroscopy (CRDS), was used to continuously analyze real-time stable isotopic composition of precipitation (Munksgaard et al., 2011). The system records a measurement every second, but we report 30 s integrated data. It consists of four major parts: a rain collection panel, a floating switch, pump, and a DS coupled to CRDS (Figure S1 in the supporting information). The rain collection panel was installed on the side of the ASE building with plastic tubing connected to the instrument in the laboratory. The system continuously analyzes reference water in a 40 L carboy when there is no rain. When it rains, rainwater collected by the panel will

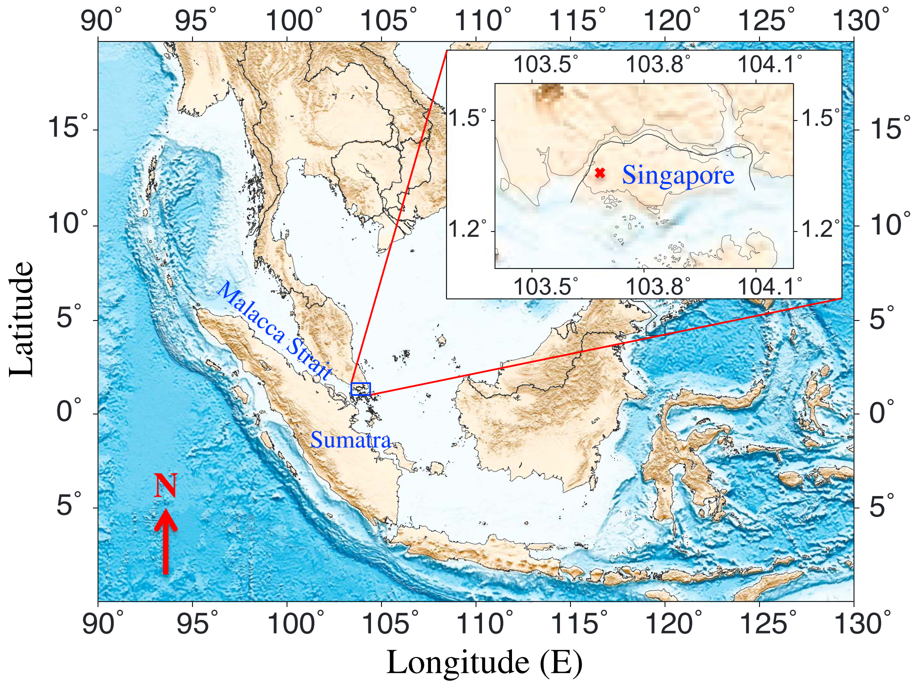


**Figure 1.** Location map of Singapore with the sampling site (1.35°N, 103.68°E, altitude of 40 m above sea level). "x" represents the sampling site.

trigger a float switch through a valve control to allow the system to analyze rainwater. The inner chamber of DS has a semipermeable expended polytetrafluoroethylene tubing to allow continuous evaporation of water samples into the chamber, and the vapor will then be introduced into CRDS for isotope analysis. We use three in-house calibration standards with $\delta^{18}O$ and $\delta^{2}H$ values ranging from 0 to −20‰ and 0 to −144‰, respectively, to calibrate the data collected from DS-CRDS system. Precision for our DS-CRDS is 0.2‰ or better for $\delta^{18}O$ and 0.4‰ for $\delta^{2}H$ based on the analysis of quality assurance (QA)/quality control (QC) sample three times each week over several months.

A PALMEX collector (Gröning et al., 2012) was installed in an open space on the roof of the ASE building to collect daily precipitation. A Picarro water analyzer L2140-*i* was used to analyze stable isotope composition of daily rain samples. We followed the procedure developed by Van Geldern and Barth (2012) for postrun corrections, including memory correction, drift correction, and calibration. Long-term precision of the analysis is 0.04‰ for $\delta^{18}O$ and 0.2‰ for $\delta^{2}H$ based on our in-house QA/QC water standards analyzed over years.

### 2.3. Meteorological Data

Air temperature, relative humidity (RH), and rain intensity on-site were monitored using a HOBO Data Logging Rain Gauge (www.onsetcomp.com). The gauge is a battery-powered rainfall data collection and recording system, which includes a HOBO Pendant Event Data Logger (HOBO microstation H21-002) with a rain gauge smart sensor S-RGB-M002 and a 12 bit temperature and RH sensor (S-THB-M002). The sensors were set to collect data at 1 min intervals.

Radar images were obtained from the National Environment Agency Singapore taken from a ground based C-band Doppler radar centered at 1.35°N and 103.97°E. The radar can detect the presence of rain up to 240 km away from the center by measuring the reflectivity and provide a visible output (radar images) every 5 min. Mean sea level pressure and horizontal winds at 850 hPa between 1981 and 2011 used in this study for analysis of the squalls are the National Centers for Environmental Prediction Climate Forecast System Reanalysis 6-hourly products with horizontal resolution of 0.5° × 0.5°. The data were downloaded from the Research Data Archive managed by the National Center for Atmospheric Research in Boulder, Colorado, USA (rda.ucar.edu). Six hour average interpolated outgoing longwave radiation (OLR) data were also from National Centers for Environmental Prediction Climate Forecast System Reanalysis and downloaded from the same site. OLR has been used as a proxy of deep tropical convection, and there is a negative correlation between OLR and convection (Gao et al., 2013; Lekshmy et al., 2014; Vimeux et al., 2011).

Climate Prediction Center Oceanic Niño Index (ONI) is the 3 month running mean sea surface temperature departures in the Niño 3.4 region (5°N–5°S and 120°–170°W). ONI is one measure of the El Niño–Southern Oscillation (ENSO) (www.cpc.ncep.noaa.gov). Pacific warm and cold periods are identified based on a threshold of ±0.5°C for ONI. Climate Prediction Center Madden-Julian Oscillation (MJO) Index 2 is the index at 100°E, closet to our study site. The data were downloaded from the same website as ONI above. MJO indices are based on extended empirical orthogonal function analysis of pentad 200 hPa velocity potential (CHI2000) anomalies equatorward of 30°N during ENSO neutral and weak ENSO winters (November–April) in 1979–2000. The Hybrid Single-Particle Lagrangian Integrated Trajectory model was used for back trajectory calculations (ready.arl.noaa.gov/HYSPLIT.php). The 4 day back trajectory analysis was performed at three levels above the ground (850 hPa, 650 hPa, and 550 hPa), and trajectories were initiated every 6 h. Cluster analysis was applied to the trajectories of the air masses each month at the level of 850 hPa using the tool provided in the Hybrid Single-Particle Lagrangian Integrated Trajectory model (Cai et al., 2017) to examine the seasonal and monthly variability of the dominant trajectory paths through time.

## 3. Sumatra Squalls

Radar images were used to identify the squalls, to track their movement, and to distinguish between convection and stratiform zones. As narrow bands of organized storms, Sumatra Squalls propagate eastward in a line (Lo & Orton, 2016) and thus can be easily recognized through the radar images (Figure 2). Distinguishing between convection cells and the stratiform zone of the squalls is based on the method proposed by Houze (1997). The radar reflectivity pattern associated with the active convection cells in plain view is a field of localized reflectivity maxima and relatively small in area. In contrast, the adjective stratiform region is widespread with horizontally homogeneous radar echo. Figure 3 is the schematic cross section of a squall system with major components and air flows.

In total, 17 Sumatra Squalls made landfall in Singapore between April and October in 2015 (Table 1). The water isotopes of a few squalls, including those on 14 April, 1 and 14 July, and 16 September, were not recorded because of instrument failure. The majority of the squalls started to form in the late afternoon or evening in Sumatra or the Malacca Straits then propagated eastward and made landfall in Singapore mainly on the second day before dawn or in the early morning but rarely in the afternoon (Lo & Orton, 2016) (Table 1). The squalls had dissipated into the SCS by the afternoon. The life cycle of a squall, therefore, was about 20 h on average or longer. Detailed evolution of a typical squall is demonstrated in Figure S2 in the supporting information.

The squall center migrates over time from the early intermonsoon (April and May) to SW monsoon (JJAS). During April and May, they tend to be centered in the middle of Sumatra, closer to Singapore, for example, the 3 May squall (Figure S3 in the supporting information). During the SW monsoon, however, the squalls mostly form in the northern part of the region (Figure S2). The shift of the central location of the squalls can be attributed to the change in the directions of prevalent winds. Between April and May, winds are weak and variable but southwesterly or westerly winds are very common though not very strong (Figure 4a). During the SW monsoon (JJAS, Figure 4b), both southeasterly and southwesterly winds are common but the southeasterly winds are becoming stronger and thus push the central location of the squalls further north. During the NE monsoon (December–March, Figure 4d), the average wind direction is northerly to northeasterly and thus the squalls rarely occur during this time period.

## 4. Results

### 4.1. Stable Isotopes of Precipitation During Individual Events of Sumatra Squalls

Initial and mean $\delta$ values of rain events, and absolute changes in $\delta$ values during all the squalls are summarized in Table 1. In general, there is a significant change in $\delta^{18}$O value of precipitation during the majority of the squalls, and the amplitude can exceed 5‰ in a single event. Initial $\delta^{18}$O values of the events also vary greatly from −0.66 to −14.41‰, larger than intraevent variation. According to the patterns of variation in precipitation $\delta^{18}$O, we can group the squalls into three classes.

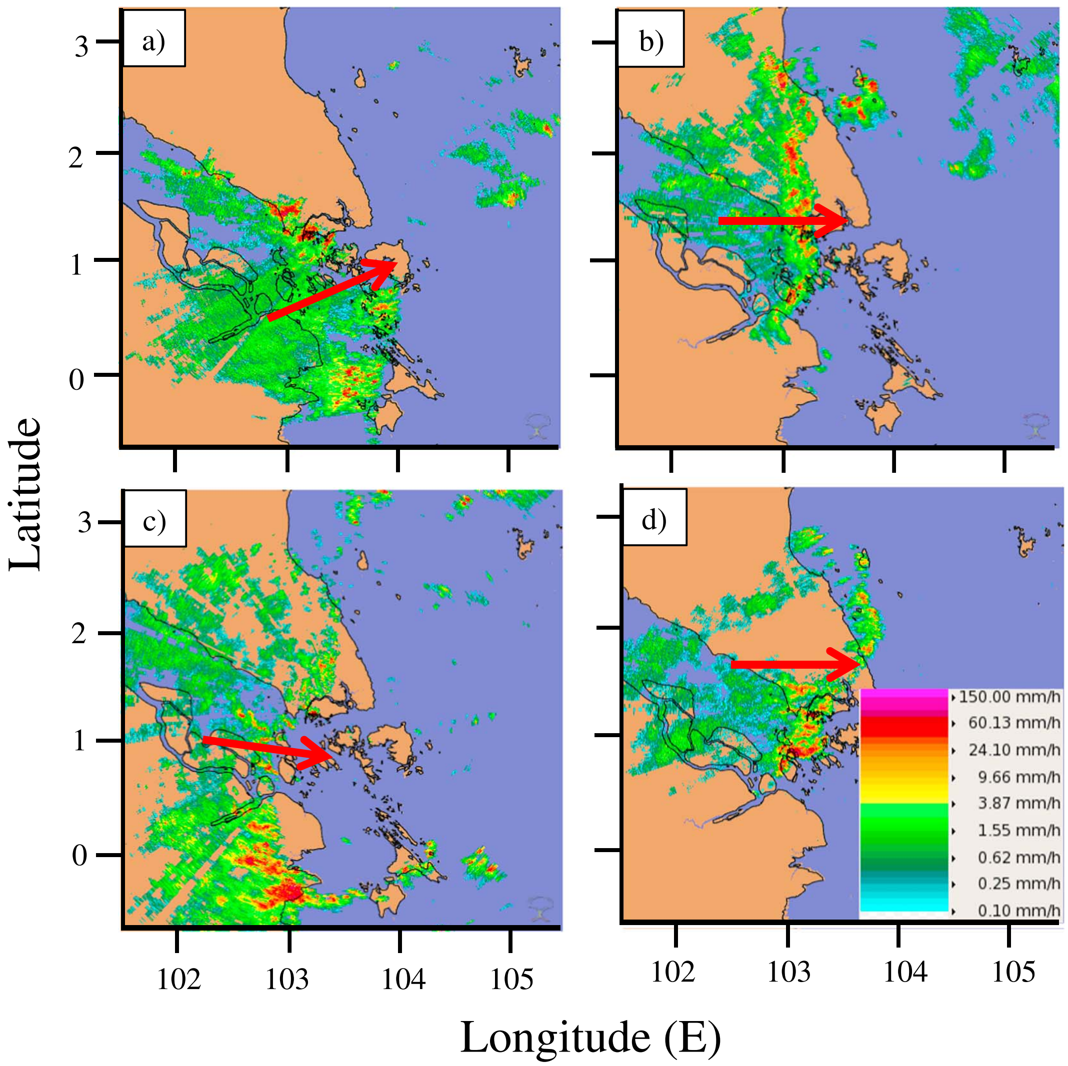


**Figure 2.** Radar reflectivity images of typical Sumatra Squalls over the sampling site at Nanyang Technological University: (a) 0042 LT 3 May 2015, (b) 0702 LT 4 July 2015, (c) 0611 LT 3 August 2015, and (d) 0247 LT 12 June 2014. Red arrow indicates the propagation direction of the squalls. Convection zone is the region with a strong horizontal color gradient, and stratiform zone is generally homogeneous in color.

In the first class, $\delta^{18}O$ values change in a V pattern (Figure 5). The value is generally high at the beginning, decreases significantly during the rain events, and gradually increases again toward to the end of the events. The lowest $\delta^{18}O$ value is normally observed at the time when the stratiform zone of the squalls moved above the station, sometimes close to the transition zone between convection and stratiform zones. The first event on 16 June 2015 is an exception because the lowest $\delta^{18}O$ value occurred in the convection portion. Surface temperature drops slightly (about 1 to 3°C) with the decrease in $\delta^{18}O$ value in the early stage, corresponding to the arrival of convective systems due to propagation of the cold pool initiated by the evaporation of falling precipitation in unsaturated downdrafts (Tremoy et al., 2014). Such small change in temperature will not significantly affect the $\delta^{18}O$ value of precipitation. Like air temperature, the RH also changes during events. In general, RH is slightly low at the beginning and the end and higher during the middle of the event. RH and air temperature data obtained from our rain gauge only reflect the conditions at the sampling site, and they do not completely represent the atmospheric conditions below the cloud base. There are some minor differences in the patterns of variation in $\delta$ value among the squalls in the first class. For a typical V pattern, its final $\delta^{18}O$ value is close to the initial value (Figure 5a). Very often at the end of the events, the $\delta^{18}O$ value stays constant with

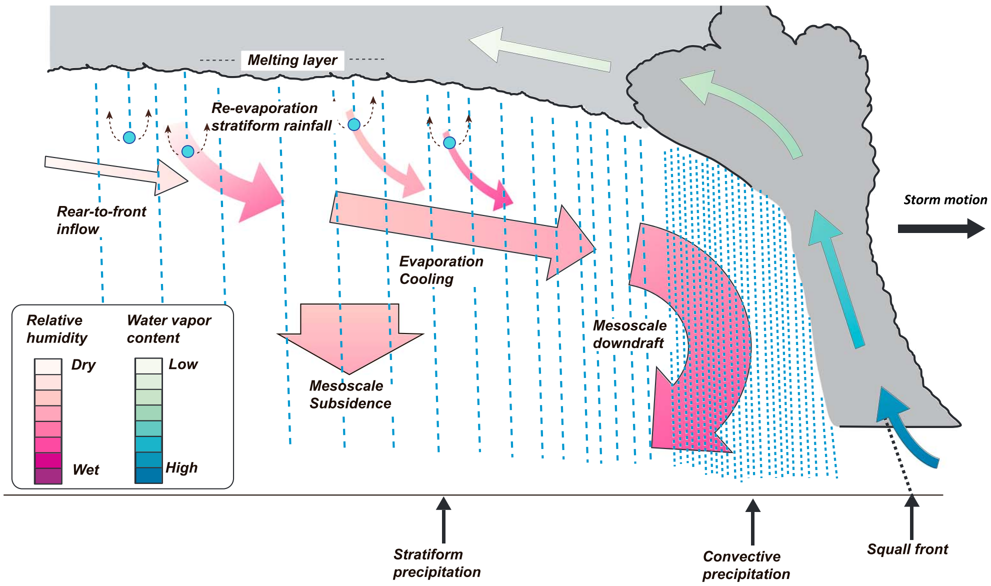


**Figure 3.** Schematic cross section of a squall system with major components and airflows.

variation being below 0.5 ‰ for several hours (Figure 5c), suggesting that the processes controlling stable isotopes of precipitation were in steady state or the height at which the rain formed was constant (Muller et al., 2015). The final $\delta^{18}O$ value could be higher than the initial (Figure 5d).

In the less common second class, the $\delta^{18}O$ value of precipitation varied in a W-shape or a two V-shape pattern (Figure 6). Both $\delta^{18}O$ value and rain amount peaks in this class fluctuated more, and the increase-decrease cycle occurred more than once during a single event. As an organized convection system, the convection zone of a squall normally contains multiple convection cells. The W-shape pattern was due to two or more convection cells passing over the sampling site. The lowest $\delta^{18}O$ value

**Table 1**
*Major Features of the Sumatra Squalls in 2015*

| Month | Date | Rain event | Isotope pattern | Start | End | Duration (min) | Rain amount (mm) | $\delta^{18}O$ value (‰,VSMOW) | | | | |
|---|---|---|---|---|---|---|---|---|---|---|---|---|
| | | | | | | | | Initial | Highest | Lowest | $\delta$ difference | Average |
| April | 19 | 1 | V | 05:05:00 | 06:25:00 | 80 | 31.2 | −5.54 | −5.54 | −9.62 | 4.08 | −8.09 |
| May | 3 | 1 | W | 00:47:00 | 05:00:00 | 253 | 86 | −8.15 | −8.15 | −11.36 | 3.21 | −9.84 |
| | 23 | 1 | Other[a] | 09:18:00 | 12:15:00 | 177 | 5 | −5.17 | −5.17 | −7.04 | 1.87 | −6.31 |
| June | 12 | 1 | V | 09:45:00 | 11:10:00 | 85 | 43 | −8.74 | −8.43 | −11.37 | 2.94 | −10.04 |
| | | 2[b] | | 13:06:00 | 14:27:00 | 81 | 2.6 | −9.52 | −8.01 | −9.92 | 0.40 | −9.20 |
| | 14 | 1 | V | 08:18:00 | 11:00:00 | 162 | 2.8 | −14.41 | −13.58 | −16.83 | 3.25 | −15.76 |
| | 16 | 1 | V | 03:05:00 | 04:20:00 | 75 | 7.2 | −6.81 | −6.09 | −7.15 | 1.06 | −6.39 |
| | | 2 | Other[a] | 07:50:00 | 07:14:00 | 9 | 0.2 | −5.55 | −5.87 | −6.06 | 0.18 | −5.97 |
| July | 4 | 1 | V | 07:11:00 | 08:55:00 | 104 | 20.4 | −4.33 | −4.14 | −7.92 | 3.78 | −5.89 |
| August | 3 | 1 | V | 06:11:00 | 07:49:00 | 68 | 57.8 | −4.89 | −4.89 | −7.26 | 2.36 | −6.56 |
| | | 2 | Other[a] | 09:11:00 | 11:15:00 | 59 | 1.2 | −6.19 | −6.11 | −7.10 | 0.99 | −6.51 |
| | 4 | 1 | V | 05:36:00 | 09:29:00 | 233 | 26 | −7.12 | −7.12 | −12.15 | 5.03 | −11.04 |
| | 6 | 1 | Other[a] | 13:28:00 | 13:53:00 | 26 | 2.2 | −3.91 | −3.06 | −3.98 | 0.92 | −3.46 |
| | | 2 | V | 14:21:00 | 15:22:00 | 61 | 26.2 | −8.05 | −6.97 | −8.74 | 1.77 | −7.83 |
| | 21 | 1 | Other[a] | 05:32:00 | 05:55:00 | 23 | 0.4 | −0.66 | −0.66 | −1.66 | 1.00 | −0.92 |
| | | 2 | V | 09:40:00 | 10:28:00 | 48 | 1.8 | −2.20 | −2.20 | −3.45 | 1.24 | −2.68 |
| September | 15 | 1 | W | 12:32:00 | 14:50:00 | 138 | 19 | −3.32 | −3.32 | −8.41 | 5.09 | −5.79 |

*Note*. VSMOW = Vienna Standard Mean Ocean Water.
[a]Only partial stratiform precipitation of the events. [b]Not related to the squall.

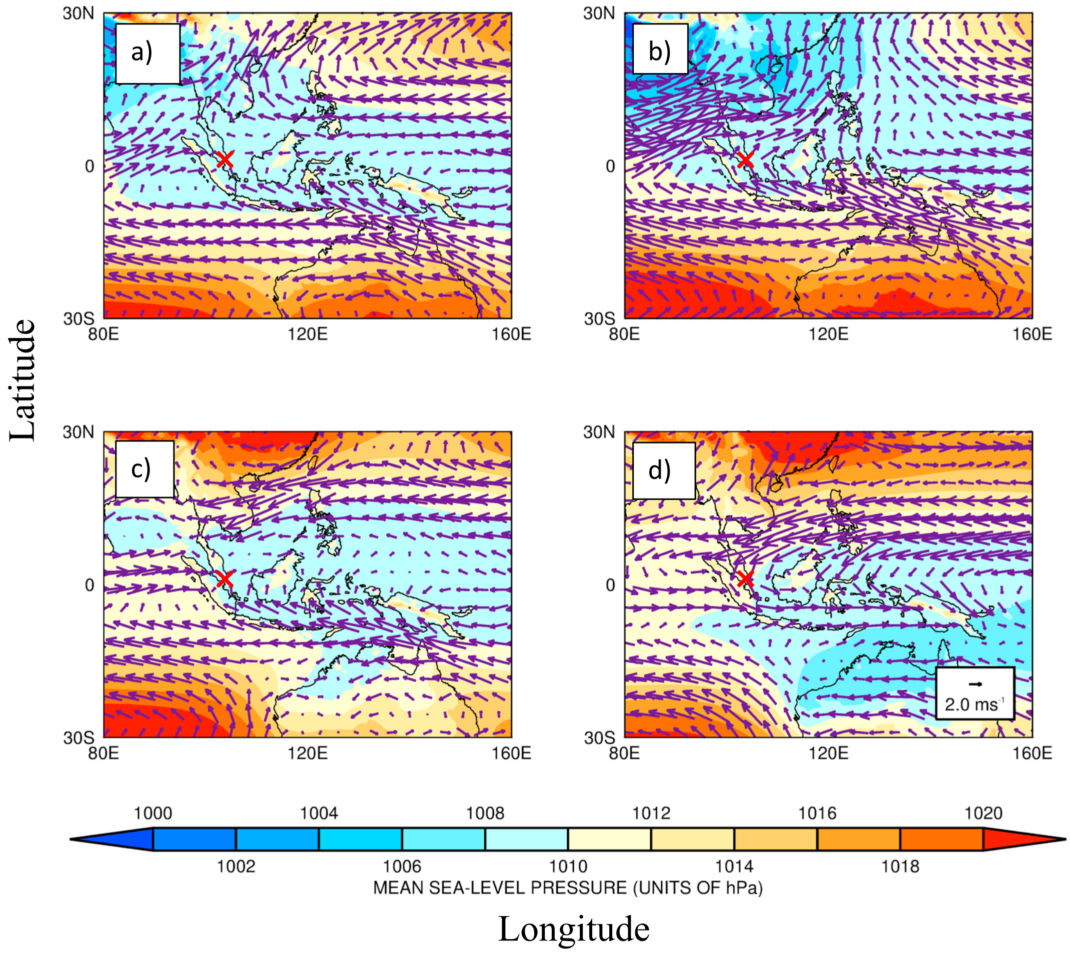


**Figure 4.** Mean sea level pressure (shading, units of hPa) and horizontal winds at 850 hPa (vectors, units of $ms^{-1}$) over 30 years between 1981 and 2010 from National Centers for Environmental Prediction reanalysis: (a) April and May, (b) June–September, (c) October and November, and (d) December–March. "x" represents the sampling site.

in a single event could occur in both the convection zone (Figure 6a) and the stratiform portion (Figure 6b) of the squalls.

In addition to the V and W shape, precipitation $\delta^{18}O$ value of the events from other squalls varies in different ways, and they are less easily classified. However, they share some characteristics establishing a third class. In this class, the very common pattern observed is that $\delta^{18}O$ value gradually increased throughout the event (Figure 7a). Another pattern is that $\delta^{18}O$ value of the precipitation did not change more than 0.5‰ (Figure 7b). Detailed examination of radar images revealed that these events are simply the stratiform part of the squalls, reflecting partial V or W pattern.

We also performed correlation analysis of $\delta^{18}O$ and d-excess with temperature and RH during the squalls (Table S1 in the supporting information). In general, there is a strong positive correlation between temperature and $\delta^{18}O$ ($r = 0.40$ to 0.92, $p < 0.001$) during the majority of events except for a few events with minimal variation in temperature, for example, the 3 May event. The lowest $\delta^{18}O$ value is generally observed at the lowest temperature during events. In contrast, there is no systematic correlation between $\delta^{18}O$ and RH and between d-excess and both temperature and RH. The correlation ranges from no correlation to positive or negative correlation from event to event. Such spurious relationships of $\delta^{18}O$ and d-excess with both temperature and RH likely suggest that stable isotopes of precipitation at the intraevent level are not controlled by the ambient environmental conditions on the ground. It is also possible that temperature and RH recorded by our rain gauge at the sampling site does not fully represent the actual atmospheric conditions below the clouds during events, especially RH.

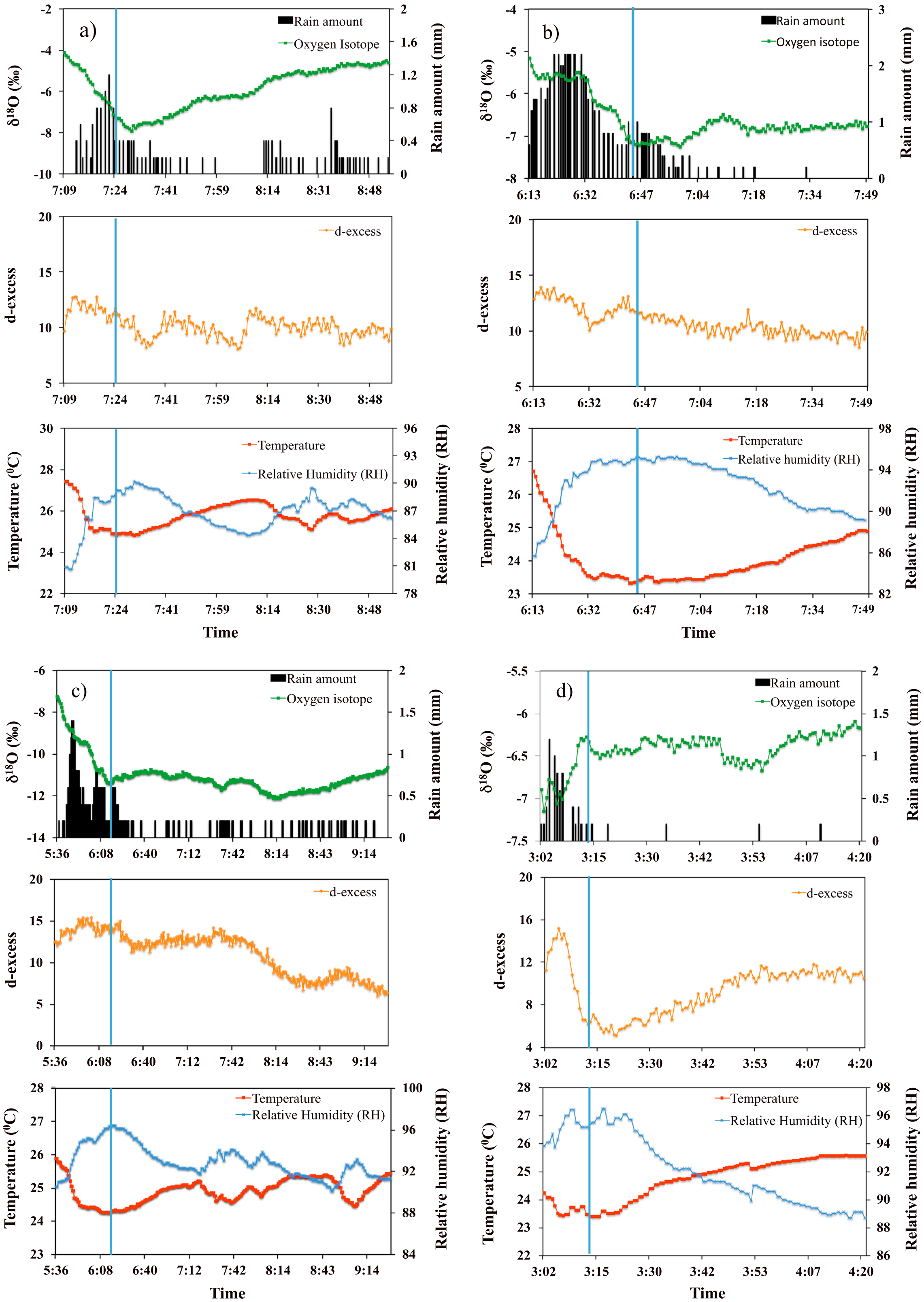


**Figure 5.** V-shape pattern of $\delta^{18}O$ values of the events (Class A) with time series of d-excess, air temperature, and relative humidity (RH) at the sampling site: (a) 4 July 2015, (b) 3 August 2015, (c) 4 August 2015, and (d) the first event of 16 June 2015. Vertical blue line divides convection zone and stratiform zone of the squalls.

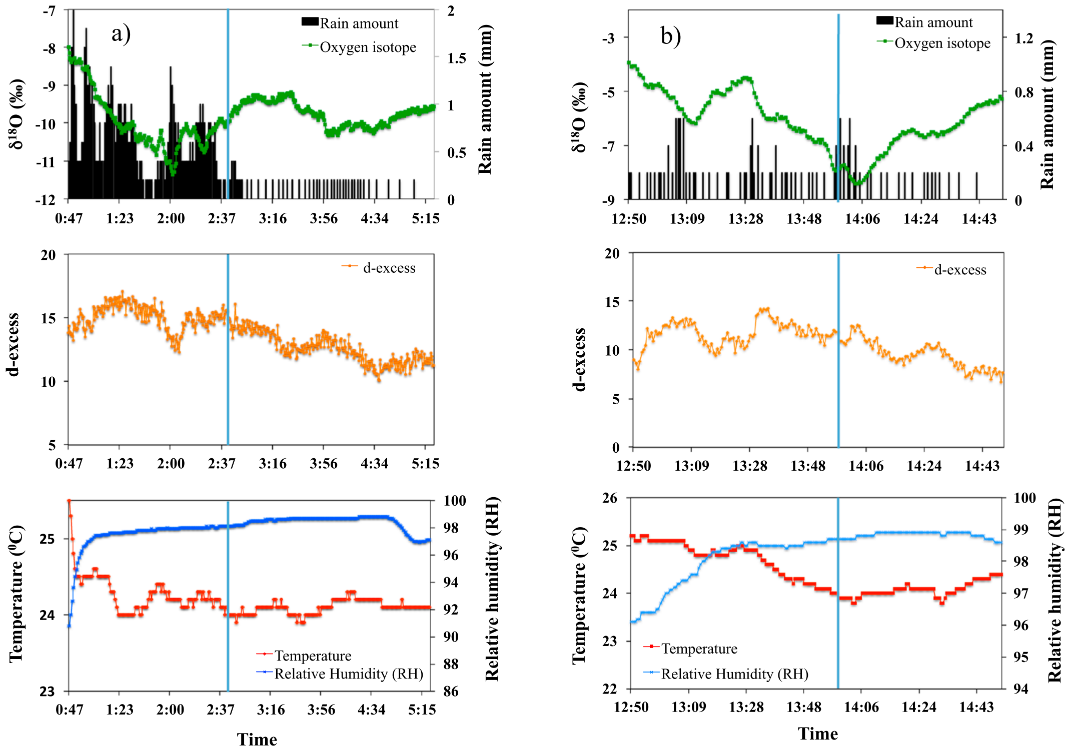


**Figure 6.** W-shape pattern of $\delta^{18}$O values of the events (Class B) with time series of d-excess, air temperature and relative humidity (RH) at the sampling site: (a) 3 May 2015 and (b) 15 September 2015. Vertical blue line divides convection zone and stratiform zone of the squalls.

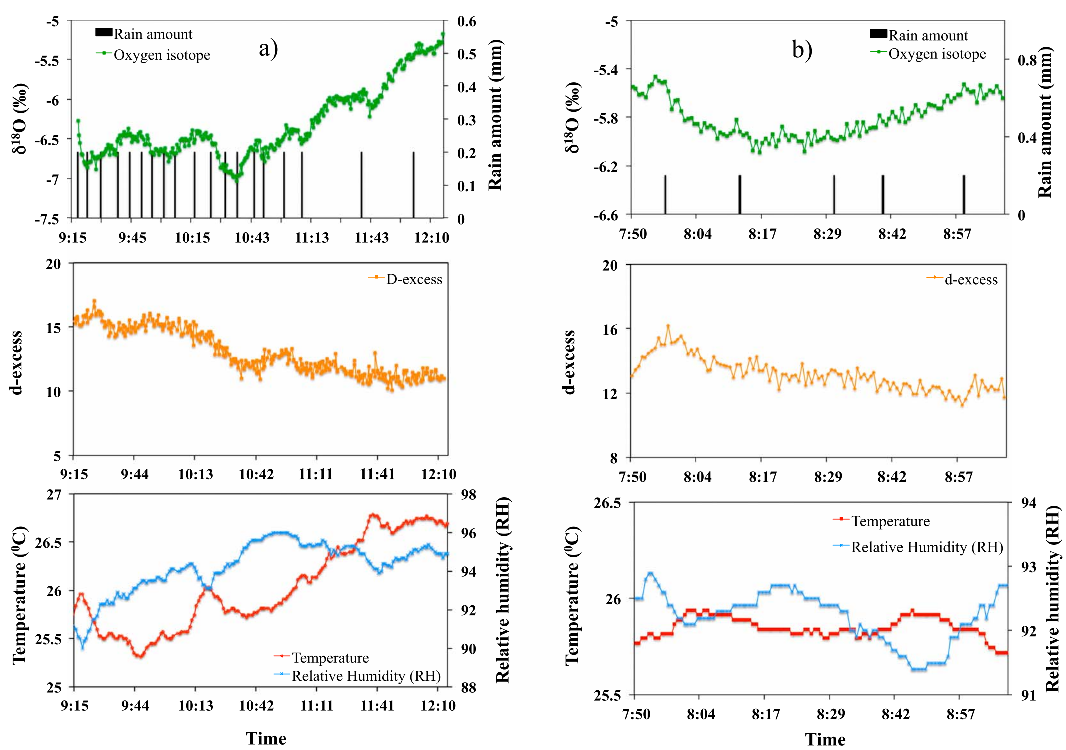


**Figure 7.** Other shape pattern of $\delta^{18}$O values of the events (Class C) with time series of d-excess, air temperature, and relative humidity (RH) at the sampling site: (a) 23 May 2015 and (b) the second event of 16 June 2015.

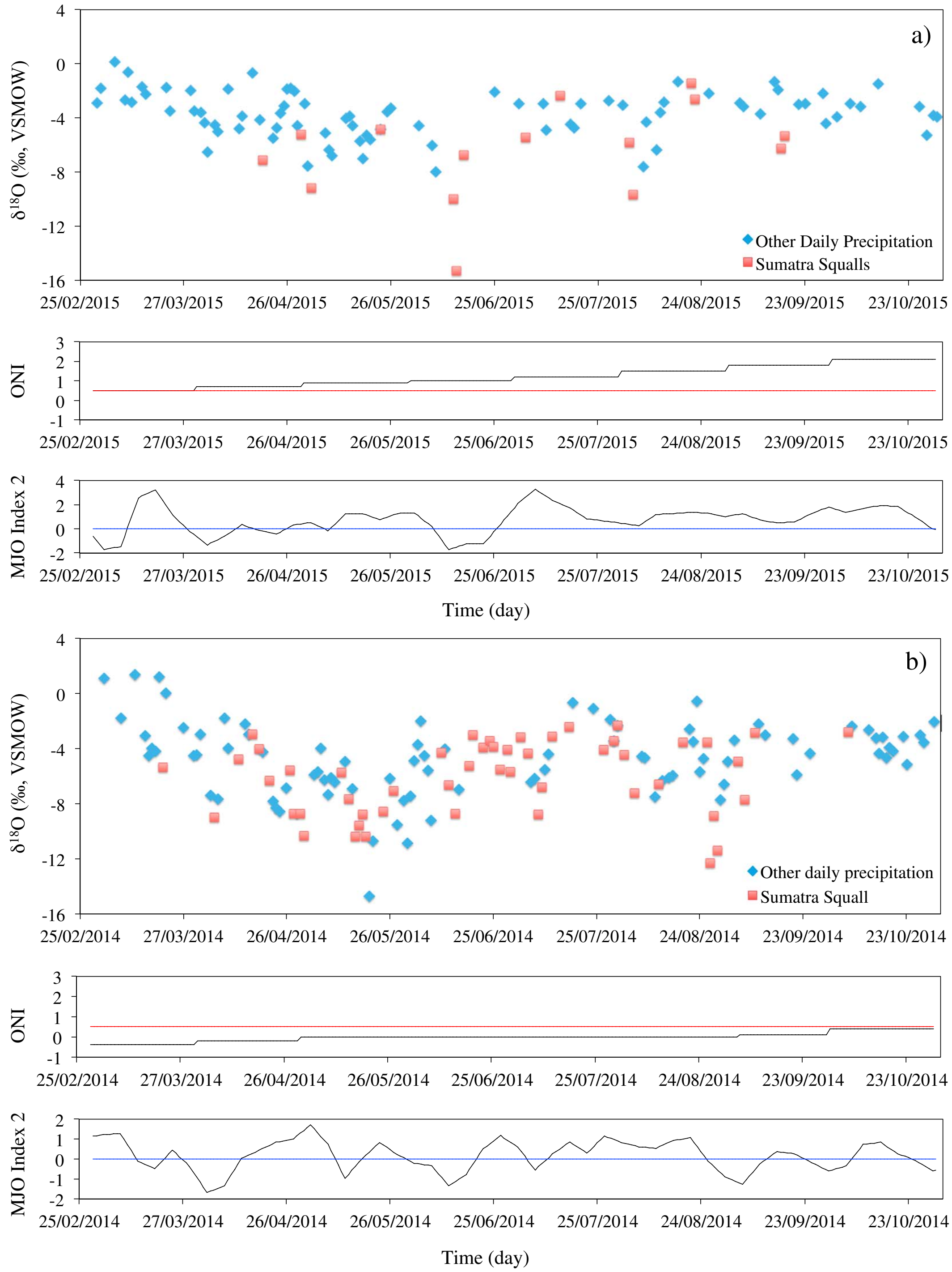


**Figure 8.** Time series of $\delta^{18}O$ values of the daily precipitation in 2015 (a) and 2014 (b) with Climate Prediction Center Madden-Julian Oscillation (MJO) Index 2 at 100°E and Oceanic Niño Index (ONI). Red square represents the precipitation related to the Sumatra Squalls. VSMOW = Vienna Standard Mean Ocean Water.

### 4.2. Stable Isotopes of Daily Precipitation

Figure 8a shows the time series of the $\delta^{18}O$ value of daily precipitation collected between March and October in 2015, an El Niño year. In comparison with a normal year, the $\delta^{18}O$ value of daily precipitation collected during the same time period in 2014 is also presented (Figure 8b). We included the MJO and ENSO indices in these figures to evaluate the relationship of the $\delta$ value of daily precipitation with MJO and ENSO. $\delta^{18}O$ values of daily precipitation are characterized by periodic shifts to more negative values, for example, to −15.31‰ on 14 June 2015. The amplitude of shift in $\delta^{18}O$ values of daily precipitation is larger than that of intraevent variation. Detailed examination indicates that these negative shifts are largely related to the squalls.

## 5. Discussion

### 5.1. Processes Controlling $\delta$ Value of Precipitation During the Sumatra Squalls

The simple explanation for the observed variation patterns of precipitation $\delta$ value is that condensation processes are the dominant factor controlling the evolution of $\delta$ values of precipitation during the squalls. Preferable removal of heavy isotopes during condensation causes the $\delta$ values of the remaining vapor to continuously decrease (Dansgaard, 1964; Gonfiantini et al., 2001; Vuille et al., 2003). Thus, the maximum depletion would be expected to occur at the maximum rain intensity. For the majority of the squalls, the lowest $\delta$ value was observed in the stratiform zone not at the maximum rain intensity, which normally occurs in the early convection zone (Figures 5 and 6). Our observations are in good agreement with the observation of mesoscale convective systems (MCSs) in the tropical regions by Risi et al. (2010) and Kurita et al. (2011). Most negative $\delta$ values observed during tropical convection have been attributed to mesoscale subsidence of isotopically depleted air in unsaturated downdraft of the stratiform region (Bony et al., 2008; Kurita, 2013; Risi et al., 2010).

In the tropics, stratiform and convective precipitation occur together within the same complex of convection systems with the stratiform covering great areas and accounting for a large portion of the tropical rainfall, up to 70–80% (Houze, 1997, 2004; Schumacher & Houze, 2003) (Figure 2). The cloud base of the stratiform zone occurs in the middle troposphere under the region of ascent because of the combined effect of layer lifting and the accumulation of older, weakening and expanding buoyant element aloft (Houze, 2004). Below the cloud base occurs a region of net descent, the mesoscale subsidence (Figure 3), which is caused by the cooling of midtropospheric environmental air by melting and evaporation of precipitation falling out of the cloud aloft. The mesoscale subsidence takes isotopically depleted vapor into the subcloud layer, which is reused or recycled for precipitation in convection (Kurita, 2013; Risi, Bony, & Vimeux, 2008; Risi et al., 2010). This also can explain that the lowest temperatures normally accompany the lowest $\delta$ value during most events because the cold air brought down cools the ambient environment. In one simulation of the evolution of stable isotopes in the squall line by Risi et al. (2010), an increase of the maximum altitude reached by low-level air parcel (equivalent to the minimum temperature encountered) from 0 km at the beginning of the line to 2.5 km in the stratiform zone leads to a strong decrease in $\delta^{18}O$ value of vapor (from −15 to −22‰) and precipitation (from −4 to −12‰). In the more intense convection with stronger convective downdrafts vapor injected into the subcloud layer through mesoscale subsidence would be more isotopically depleted. The condensation height is probably another cause for generally lower $\delta$ values of precipitation in the stratiform zone. The mesoscale updraught in the stratiform region is approximately above the 0°C isotherm (Houze, 1997), and thus, the condensate in the stratiform zone is expected to form at higher altitude than in the convective zone.

If the mesoscale subsidence were the dominant factor for variation in $\delta^{18}O$ values observed in the stratiform in the squalls, we would expect the values to stay very low relative to the convective rains throughout the events. In many cases, however, $\delta^{18}O$ values gradually increase with time after the minimum value is reached in the stratiform zone and can be higher than the initial convective rainfall at the end of events (Figures 5 and 6). Reevaporation and isotopic equilibrium of rain with ambient vapor under the cloud base likely play an important role to modify the $\delta^{18}O$ value, especially near the end of these events.

In the stratiform zone for the most events, d-excess values of the precipitation exhibit a corresponding decrease with an increase in $\delta^{18}O$ values toward the end of events. There is an inverse relationship existing between $\delta^{18}O$ values and d-excess ($r = -0.6$ to $-1$, $p < 0.001$), specifically in the last stage of the stratiform zone (Table S2 in the supporting information). The $\delta^{18}O$ and $\delta^2H$ values of the precipitation in the stratiform zones normally define an evaporation line with a different slope relative to the local meteoric water line (LMWL) in Singapore (Figure 9). In the convection zone, however, the inverse relationship between $\delta^{18}O$ values and d-excess is much weaker ($r = 0$ to $-0.3$, $p < 0.01$) with a few having higher but much less

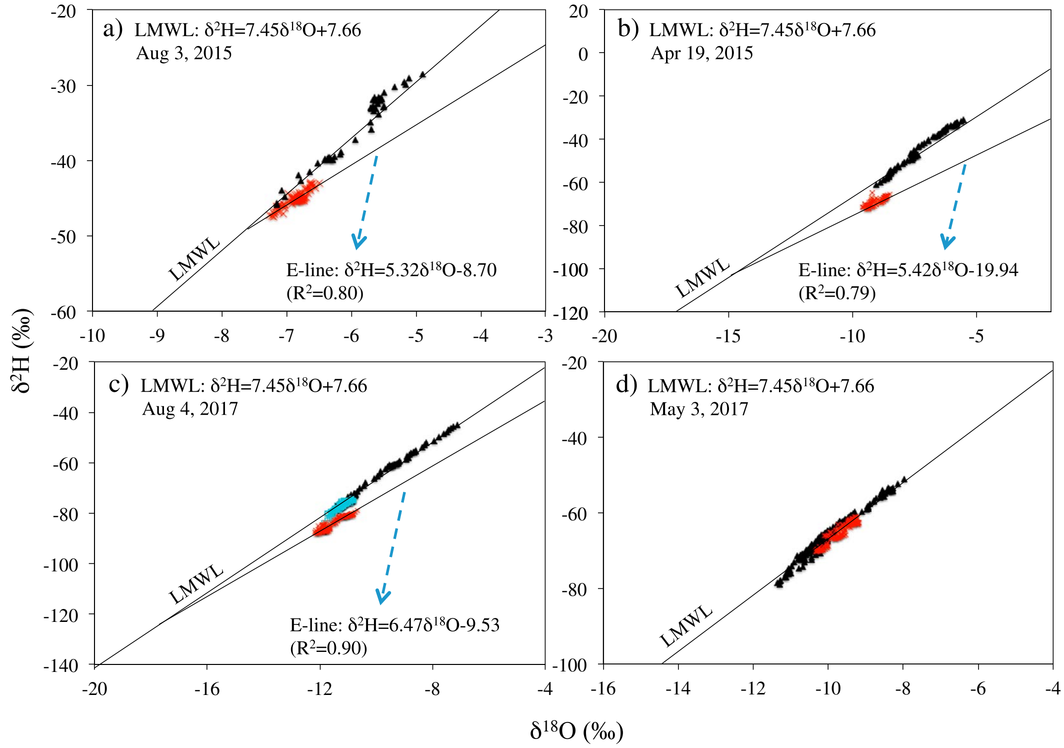


**Figure 9.** Plots of $\delta^{18}$O versus $\delta^{12}$H of the precipitation during the Sumatra Squalls at Nanyang Technological University sampling site: (a) August 2015, (b) 19 April 2015, (c) 4 August 2015, and (d) 3 May 2015. Black triangle = precipitation from convection zones; red cross = precipitation from stratiform zone; blue cross in (c) = the early part of the stratiform zone; E-line = evaporation line. Singapore local meteoric water line (LMWL) is from He et al. (2015).

significant correlation (Table S2). During some events, d-excess varies in the same way as $\delta^{18}$O values, and thus, there is a positive correlation between them ($r$ = +0.6 and 0.05, $p < 0.001$ and = 0.1, respectively), for example, the events on 19 April and 4 July. $\delta^{18}$O and $\delta^{2}$H values of the precipitation in the convection zone normally plot closely along the LMWL instead of along an evaporation line, suggesting insignificant reevaporation of raindrops in the convection zones. During the event on 4 August, reevaporation was very weak for the first 2 h of the stratiform zone, and there is no correlation between $\delta^{18}$O values and d-excess, but in the last hour, significant reevaporation was observed as indicated by a stronger correlation between $\delta^{18}$O values and d-excess ($r = -0.6$, $P < 0.001$). Therefore, the $\delta^{18}$O and $\delta^{2}$H values of the precipitation during the first 2 h plot closely to the LMWL, and in the last hour, they plot along an evaporation line (Figure 9c). Rain reevaporation could be minimal throughout the whole event as in 3 May, when the $\delta^{18}$O and $\delta^{2}$H values of the precipitation in both convection and stratiform zones plot along the LMWL (Figure 9d). There is no correlation existing between the $\delta$ value and d-excess of the precipitation in this event.

Physically, reevaporation is important when RH is low, and diffusive exchanges enable the raindrops to reequilibrate with the vapor when RH is high (Bony et al., 2008; Lee & Fung, 2008; Tremoy et al., 2014). Raindrop size and rain rate or intensity also affect the reevaporation (Lee & Fung, 2008). In the convection zone, the rain intensity was high and the maximum intensity was generally observed in this zone (Figure 3), and the raindrop size was large on average (Lee & Fung, 2008; Rao et al., 2008). Therefore, the reevaporation of raindrops was in general weaker in the convection zone. Within the stratiform, rain intensity dropped, RH decreased, and raindrop size was also relatively small, especially in the later period of events. In MCSs like Sumatra Squalls, there exists a middle-level rear-front inflow that feeds the mesoscale downdraft (Figure 3). It is believed that evaporation, melting, and sublimation in the stratiform region all contribute substantially to the evolution and strength of the rear-front inflow (Houze, 2004). This airflow is characterized by dry conditions and gradually becomes wet due to reevaporation of raindrops under the stratiform cloud deck. Therefore, the middle-level inflow at the left edge is completely dry and thus heavy reevaporation may occur at this region, resulting in heavy oxygen isotope enrichment, normally at the late stage of the stratiform zone. Different degrees of rain reevaporation observed during the events are very likely related to various RH conditions in the subcloud environment. Throughout the whole event on 3 May, minimal reevaporation of raindrops can probably be attributed to high RH. High-resolution, vertical profiles of humidity are needed to evaluate the effects of reevaporation and moisture isotope exchange in the subcloud layer.

No significant variation in $\delta^{18}O$ values (<0.5‰) is observed in the stratiform zone of the event on 16 June, although there is a slight increase near the end (Figure 5d). In contrast, there is a gradual increase in d-excess throughout the stratiform zone, and there is no correlation existing at all between d-excess and $\delta^{18}O$ values. This observation can be attributed to either an unknown process that might have caused the increase in d-excess without significant change in $\delta^{18}O$ values or the replenishment of moisture from the ambient environment. Fresh moisture might have similar stable isotopic values with vapor but with different d-excess. Lee and Fung (2008), Yoshimura et al. (2010), and Tremoy et al. (2014) have recognized the influence of moisture refreshment on the stable isotopes of precipitation.

The squalls on 3 May (Figure 6a) and 16 June (Figure 5d) are unique in that the evolution of their $\delta$ values are different from the others although they present the similar variation pattern. These two squalls have some features in common: (1) rainfall largely occurred in the convection zone. For example, 90% of the rainfall from the 16 June event occurred in the first 10 min in the convection zone, while the rain intensity in the stratiform zone was extremely low; (2) the lowest $\delta$ values were observed in the convection zone; (3) in general, the stratiform has higher and constant $\delta$ values than the convection zone. It seems that extremely intensive rain at the very early stage of these events significantly depleted the $\delta^{18}O$ value of vapor, thus leading to the very negative $\delta^{18}O$ value of precipitation in the convection core.

### 5.2. Contribution to the Variation in $\delta^{18}O$ Values of Daily Precipitation

Moisture sources have been considered a major cause for the change in $\delta^{18}O$ value of precipitation in many locations, specifically in high-latitude regions (e.g., Theakstone, 2011; Vreča et al., 2007). To investigate the moisture sources of precipitation, we performed backward trajectory analysis for the time period when the squalls are prevalent (Figure S4 in the supporting information) and cluster analysis of trajectories in each month (Figure S5 in the supporting information). The analysis indicates that the Java Sea and the Indian Ocean are the two major moisture sources of precipitation in our study area, and the minor contribution comes from the local SCS and the Malacca Strait, mostly during the early intermonsoon time. Relative to 2014, the moisture source from the Java Sea became more dominant over the Indian Ocean in 2015 due to the weak SW monsoon during El Niño. The results of back trajectory analysis are in agreement with atmospheric reanalysis of horizontal winds in the study area (Figure 4). However, change in moisture sources can only introduce minimal variation to $\delta^{18}O$ values of precipitation because there is no significant difference in ocean water isotopes and ambient conditions in these source regions, including surface temperature and RH (Benetti et al., 2014; LeGrande & Schmidt, 2006; Majoube, 1971). It is the physical processes in clouds that modify vapor isotopes.

We believe that these periodic shifts to more negative values in daily precipitation during the study period are largely associated with Sumatra Squalls. The amplitude of such negative shifts can be more than 10‰. In individual events, the absolute change in $\delta^{18}O$ values varies from about 1‰ to more than 5‰ during the squalls (Table 1), showing the different influence of individual squalls on the $\delta^{18}O$ value of precipitation likely due to their different dynamic conditions, including different speeds of convective uplift, amount condensation, and other physical processes in convection clouds. The squalls related to the events with minor variation in $\delta^{18}O$ values are dynamically weak in general, either small in scale or only portions made landfall at the sampling site. The intraevent variation in $\delta^{18}O$ values at the sampling site cannot fully explain the negative shifts in $\delta^{18}O$ values of daily precipitation, especially those shifts of more than 10‰.

Our DS recorded variable initial $\delta^{18}O$ values of individual rain events during the squalls, from −0.66‰ to −14.41‰ (Table 1). Highly variable initial $\delta$ values also suggest variable $\delta$ values of the initial vapor or air masses because the initial $\delta$ values of individual events should largely reflect the initial air mass or vapor from which precipitation originated (Conroy et al., 2016; Lee & Fung, 2008; Risi et al., 2010). In general, those events with very low $\delta$ values also have low initial values. For example, the event with the lowest $\delta^{18}O$ value (−16.83‰) observed during the squall on 14 June also has the lowest initial $\delta^{18}O$ value (−14.41‰), and

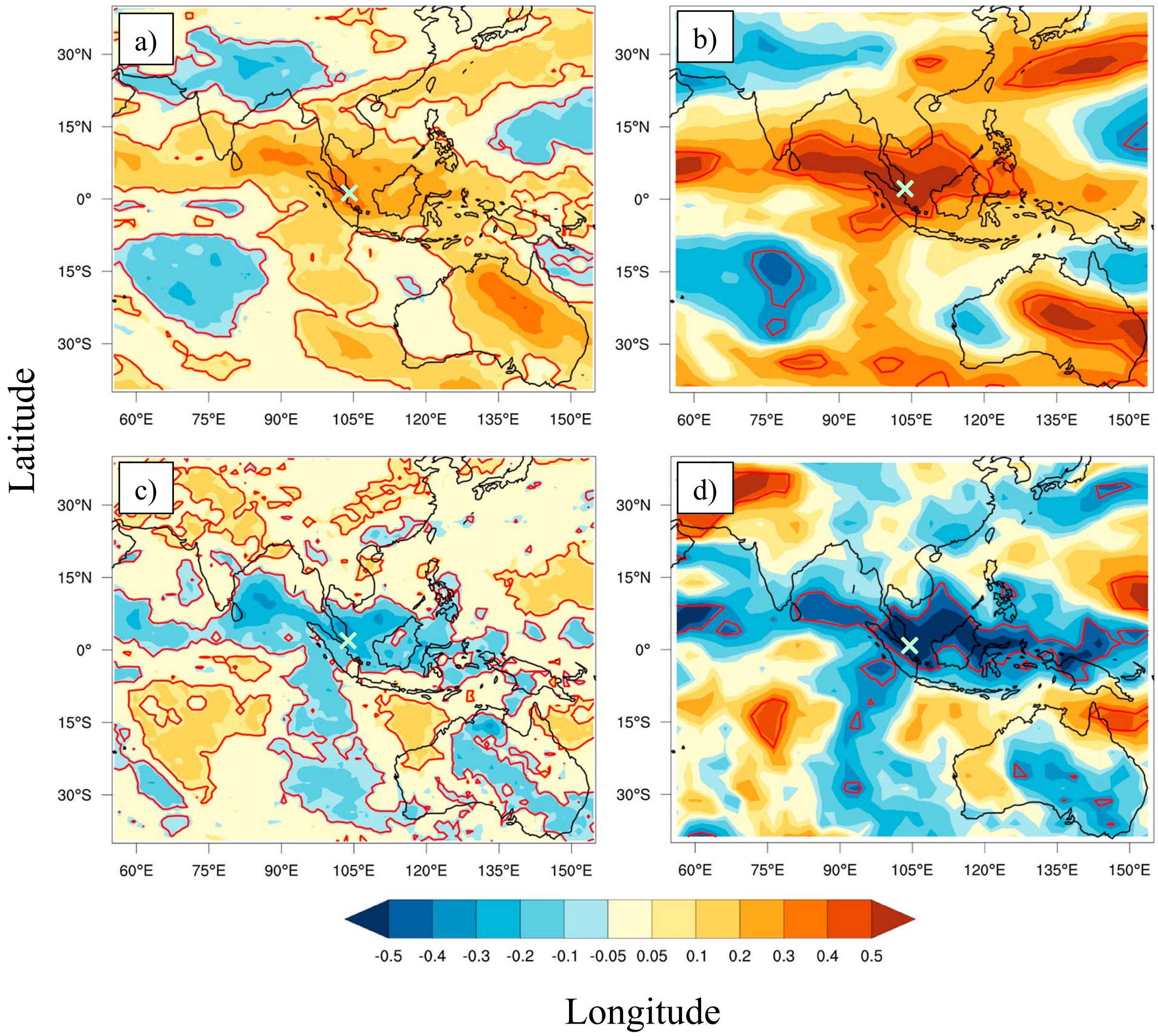


**Figure 10.** Correlation map of $\delta^{18}O$ value of daily precipitation with (a) gridded outgoing longwave radiation and (c) rainfalls, and monthly mean $\delta^{18}O$ value of precipitation with (b) gridded outgoing longwave radiation and (d) rainfalls in the study area. "x" represents the Nanyang Technological University sampling site. Red contour lines indicate the area of 90% confidence level.

thus, the moisture or vapor in the clouds already had very low isotope values prior to our sampling site. Therefore, the $\delta$ value in the initial vapor of these rain events should largely represent the past convective activities in the squalls prior to the site. Zwart et al. (2016) investigated the stable isotopes of precipitation during the Australian monsoon and found a strong relationship between isotopic variation and the integrated rainfall amount of air masses prior to arriving at the measurement locations. Most recently, backward trajectory analysis of moisture sources of precipitation in the Asian summer monsoon region suggests upwind convection rather than moisture source is the cause of interannual variability in $\delta^{18}O$ of Asian summer monsoon precipitation (Cai et al., 2017). Control of the integrated or accumulative convection activity over precipitation $\delta^{18}O$ value has also been inferred in several other studies (Cai et al., 2017; Gao et al., 2013; Kurita, 2013; Moerman et al., 2013; Risi, Bony, Vimeux, Descroix, et al., 2008; Vimeux et al., 2011). These studies have noted that isotopic values of surface moisture reflect the past several days' history of convective activity from the upwind region. We can reasonably conclude that the stable isotope compositions of daily precipitation represent current convection and largely past convection activities in the squalls prior to on-site events.

Regional regression map shows a strong correlation between $\delta^{18}O$ values of daily precipitation and OLR in the region, including the Bay of Bengal, the Indonesian archipelago, the Malay Peninsula, the SCS, and the western Pacific (Figure 10a). The correlation is stronger with monthly $\delta^{18}O$ values of precipitation (Figure 10b). The similar but inverse relationship is observed between the regional rainfall and $\delta^{18}O$ values of precipitation (Figures 10c and 10d) although the $\delta^{18}O$ value of daily precipitation has no correlation with the rain amount at the sampling site (He et al., 2015). Such correlations simply imply that the $\delta^{18}O$ value of daily precipitation in the study area is closely related to the regional organized convections in the whole region. Stronger regional organized convection leads to more negative $\delta^{18}O$ values of precipitation with higher rainfall and vice versa. A correlation between the Asian monsoon and the formation of Sumatra Squalls is apparent. Unlike the regional organized convection, that is, Sumatra Squalls, local convection has limited impact on the $\delta^{18}O$ value of daily precipitation, as reflected by the much smaller variation in both initial $\delta^{18}O$ value and intraevent variation of related rain events (Table S3 in the supporting information). Therefore, regional organized convective system like Sumatra Squalls are likely one major driver of variation in $\delta^{18}O$ value of daily precipitation during the intermonsoon and SW monsoon in the region.

The frequency of Sumatra Squalls in 2015 is much lower than in 2014 (Table S4 in the supporting information). Fifty squalls made landfall in Singapore between April and October in 2014, an average number of the squalls observed in a normal year (Lo & Orton, 2016), but only 17 squalls passed the sampling site during the same time period in 2015. Correspondingly, the frequency of negative shifts in the $\delta^{18}O$ value of daily precipitation is also lower in 2015 than in 2014 (Figure 8). As a result, the $\delta^{18}O$ value (weighted average) of precipitation during the SW monsoon and intermonsoon periods in 2014 is generally lower (>1‰) than in 2015. The lower frequency of the squalls in 2015 can be attributed to El Niño. The ONI shows that the tropical pacific warm period started before 2015 (Figure 8b), and ONI reached above 2 during the 2015–16 NE monsoon. Previously, during El Niño years, the frequency of squalls declined; for example, only 11 squalls were recorded in the 1997–1998 El Niño year (J. C. F. Lo, personal communication, at Center for Climate Research Singapore, 2017). During an El Niño event, convection over the western Pacific warm pool and the Asian monsoon region is suppressed, resulting in a weakened monsoon and frequent droughts in the maritime continent (Chakraborty & Krishnamurti, 2003; Kane, 1997; Li & Ting, 2015). A Hovmöller diagram (Figure S6 in the supporting information) of OLR demonstrates that deep convection clouds over Singapore became much less frequent during the SW monsoon and intermonsoon seasons in 2015 relative to 2014, indicating drier conditions during the 2015 El Niño event.

The Madden-Julian Oscillation (MJO) is the dominant component of the intraseasonal variability in the tropics and propagates eastward around the global tropics with a cycle on the order of 30–60 days (Madden & Julian, 1972; Tang & Yu, 2008). One would expect that the MJO might trigger the formation or enhance the occurrence of the Sumatra Squalls in the study area. However, there is no correlation between the frequency of the squalls and the MJO activities in the study area (Figure 8). In 2014, the frequency of the squalls during the enhanced convection phase of the MJO is similar to that during the suppressed convection phase of the MJO. The highest number of the squalls was observed in July 2014 when the area was in the suppressed convection phase of the MJO. MJO might increase the intensity of the squalls but our data shows no such correlation.

## 6. Perspectives

The mesoscale subsidence of isotopically depleted air and reevaporation of falling rain below the cloud base are currently considered the two major processes that control the $\delta^{18}O$ value of precipitation during convection. However, they cannot completely explain the isotope patterns of rain events observed in this study, specifically the change in $\delta^{18}O$ value in the late event stage without decrease in d-excess. Other processes, such as the entrainment of fresh ambient air, have been proposed to explain this phenomenon. Simultaneous measurements of isotopic compositions in vapor and precipitation would provide invaluable information to evaluate the role of reevaporation and exchange of rain with the environment below the cloud base.

Although Sumatra Squalls are the most common weather phenomena occurring in the region during the SW monsoon and intermonsoon seasons, there are limited studies to investigate the squalls (Yi & Lim, 2007; Lo & Orton, 2016). The frequency of the Sumatra Squalls significantly dropped in 2015, an El Niño year. This suggests that ENSO may have an impact on the factors or processes that control the formation of the squalls. Understanding how the squalls form will help us to understand the relationship between the squalls and ENSO. Reanalysis of atmospheric conditions in the region, such as moisture and wind changes in 2015 in comparison with non–El Niño years, might provide some insights into the formation of the squall lines.

## 7. Conclusions

Continuous monitoring of stable isotopic composition of precipitation using DS-CRDS provides insights into the evolution of the stable isotopes of precipitation during Sumatra Squalls. In general, $\delta$ value of precipitation tends to be higher at the beginning and the end of the rain events with the lowest values in the middle, displaying most commonly a V shape and sometimes a W shape. Other isotopic trends observed are associated most commonly with the last stage of squalls. The amplitude of variation in $\delta^{18}O$ value of precipitations during single events is on the order of 1 to 6‰.

In most cases, the lowest $\delta^{18}O$ value is observed in the stratiform zone not during maximum rain intensity in the convection zone. This observation is in agreement with previous observations of the tropical MCSs. The mesoscale subsidence brings isotopically depleted vapor into the subcloud layer, which is reused or recycled for precipitation in convection. Our data also indicate that reevaporation of raindrops can significantly affect the stable isotopes of precipitation. In general, rain reevaporation is much stronger, especially in the last stage of the stratiform zone than in the convection zone, as indicated by the strong correlation between $\delta^{18}O$ value and d-excess in the stratiform zone relative to the convection zone. The $\delta$ values of precipitation from the convection zone mostly plot along the Singapore LMWL, while those from stratiform zone, especially near the end of an event, plot along an evaporation line with a different slope from the LMWL. Therefore, reevaporation in convection is insignificant relative to the stratiform zone during events. The RH under the cloud base likely controls the varied degree of reevaporation during rain events. High-resolution vertical profiles of RH and vapor isotopes can help to evaluate reevaporation processes.

Our current data and understanding of the physical processes that control the evolution of stable isotope of precipitation during tropical convection, however, cannot fully explain the evolution of stable isotopes of precipitation in some events. For example, there is no correlation between $\delta^{18}O$ value and d-excess or there is a positive correlation between d-excess with variation in the $\delta^{18}O$ value in the stratiform zone of some events. This suggests that other unknown processes or the process such as the refreshment of moisture likely have some control on the $\delta$ value of the precipitation during some events.

The $\delta$ values of daily precipitation collected during the SW monsoon and intermonsoon seasons in the study area fluctuate significantly with periodic shifts to more negative values. Analysis of moisture source and theoretical consideration indicate that moisture source change likely has minimal contribution to such isotopic variability in daily precipitation during study period. These negative shifts are associated with large regional convection systems such as Sumatra Squalls. The amplitude of the negative shift in $\delta^{18}O$ values of daily precipitation, however, cannot be explained by intraevent variation. Initial $\delta^{18}O$ values of precipitation in individual events during squalls are highly variable and in addition, those events with very low isotopic values also have very low initial values, implying that convective activities in the upwind region of squalls prior to the sampling site have more influence on the $\delta^{18}O$ values of precipitation. Our observation confirms previous hypotheses that integrated convection activities significantly affect the variability of $\delta^{18}O$ values of tropical precipitation. Local convection is isolated, and related rain events have much less variability in initial $\delta^{18}O$ values and intraevent variation. Local convection, therefore, has much less impact on the $\delta^{18}O$ values of the daily precipitation than regional organized convection. The significant correlation of $\delta^{18}O$ values of daily precipitation at the sampling site with regional OLR and rainfall also suggests that regional organized convection is a possible major driver for $\delta^{18}O$ values of daily precipitation during intermonsoon and SE monsoon seasons in the region.

There are only 17 squalls that made landfall in Singapore in 2015 compared to 50 observed in the study area in 2014. The drop in the frequency of the squalls can be attributed to El Niño, the warm ENSO event in 2015. During an El Niño event, regional convection shifts from the western Pacific to the central and eastern Pacific, and convection in the western Pacific and Asian monsoon region is depressed. Therefore, ENSO is probably a control of interannual variation in $\delta^{18}O$ value of the precipitation in the study area. However, the current study only spans one El Niño event in 2015 without La Niña events. The impact of ENSO on the squalls and the mean annual stable isotope compositions of precipitation needs further investigation of the long-term precipitation in the region, which will be addressed in our future studies. The occurrence of the squalls shows no correlation with MJO in the region, suggesting that MJO probably has minimal influence over their formation.

**Acknowledgments**
Authors would like to thank Ricardo Morais Fonseca for sharing his knowledge on atmospheric sciences with us without reservation. Ricardo Fonseca and Dhrubajyoti Samanta helped to make the reanalysis figures. Ng Sin Hwee, Peter Polivka, Edwin Sia, Elise Onyi, Sebastian Cantarero, Danica Linda Mancenido, Gustian Prayogi, and Muti Fardiyah helped to collect rain samples and occasionally looked after the operation of DS system. Kyle Niezgoda wrote the software and processed DS data. Dominik Jackisch helped to process DS data and make some figures on back trajectories. Three anonymous reviewers are thanked for their constructive suggestions for improving the manuscript. This research is supported by the National Research Foundation Singapore and the Singapore Ministry of Education under the Research Centres of Excellence initiative and by the National Research Foundation Singapore under its Singapore NRF Fellowship scheme (National Research Fellow Award NRF-RF2012-03). It comprises Earth Observatory of Singapore contribution 187. This research is also the part of IAEA Coordinated Research Project (CRP Code: F31004) on "Stable isotopes in precipitation and paleoclimatic archives in tropical areas to improve regional hydrological and climatic impact model" with IAEA Research agreement 17980. Isotope data and the corresponding rain gauge data are available at https://figshare.com/s/ff0980f1405f8eb6670f, and radar images are available at https://figshare.com/s/7878dbd602881ea17469.

## References

Aggarwal, P. K., Fröhlich, K., Kulkarni, K. M., & Gourcy, L. L. (2004). Stable isotope evidence for moisture sources in the Asian summer monsoon under present and past climate regimes. *Geophysical Research Letters*, *31*, L08203. https://doi.org/10.1029/2004GL019911

Barras, V., & Simmonds, I. (2009). Observation and modeling of stable water isotopes as diagnostics of rainfall dynamics over southeastern Australia. *Journal of Geophysical Research*, *114*, D23308. https://doi.org/10.1029/2009JD012132

Benetti, M., Reverdin, G., Pierre, C., Merlivat, L., Risi, C., Steen-Larsen, H. C., & Vimeux, F. (2014). Deuterium excess in marine water vapor: Dependency on relative humidity and surface wind speed during evaporation. *Journal of Geophysical Research: Atmospheres*, *119*, 584–593. https://doi.org/10.1002/2013JD020535

Bonne, J. L., Masson-Delmotte, V., Cattani, O., Delmotte, M., Risi, C., Sodemann, H., & Steen-Larsen, H. C. (2014). The isotopic composition of water vapour and precipitation in Ivittuut, southern Greenland. *Atmospheric Chemistry and Physics*, *14*(9), 4419–4439. https://doi.org/10.5194/acp-14-4419-2014

Bony, S., Risi, C., & Vimeux, F. (2008). Influence of convective processes on the isotopic composition ($\delta^{18}O$ and $\delta D$) of precipitation and water vapor in the tropics: 1. Radiative-convective equilibrium and Tropical Ocean-Global Atmosphere-Coupled Ocean-Atmosphere Response Experiment (TOGA-COARE) simulations. *Journal of Geophysical Research*, *113*, D19306. https://doi.org/10.1029/2008JD009942

Bowen, G. J. (2008). Spatial analysis of the intra-annual variation of precipitation isotope ratios and its climatological corollaries. *Journal of Geophysical Research*, *113*, D05112. https://doi.org/10.1029/2007JD009295

Cai, Z. Y., Tian, L., & Bowen, G. J. (2017). ENSO variability reflected in precipitation oxygen isotopes across the Asian summer monsoon region. *Earth and Planetary Science Letters*, *475*, 25–33. https://doi.org/10.1016/j.epsl.2017.06.035

Chakraborty, A., & Krishnamurti, T. N. (2003). A coupled model study on NESO, MJO and Indian summer monsoon rainfall relationships. *Meteorology and Atmospheric Physics*, *84*(3-4), 243–254. https://doi.org/10.1007/s00703-002-0601-7

Conroy, J. L., Noone, D., Cobb, K. M., Moerman, J. W., & Konecky, B. L. (2016). Paired stable isotopologues in precipitation and vapor: A case study of the amount effect within western tropical Pacific storms. *Journal of Geophysical Research – Atmospheres*, *121*(7), 3290–3303. https://doi.org/10.1002/2015JD023844

Dansgaard, W. (1964). Stable isotopes in precipitation. *Tellus*, *16*, 436–468.

Dansgaard, W., Johnsen, S. J., Clausen, H. B., Hvidberg, C. S., & Steffensen, J. P. (1993). Evidence for general instability of past climate from a 250-kyr. *Nature*, *364*(6434), 218–220. https://doi.org/10.1038/364218a0

Gao, J., Masson-Delmotte, V., Risi, C., He, Y., & Yao, T. (2013). What controls precipitation $\delta^{18}O$ in the southern Tibetan Plateau at seasonal and intra-seasonal scales? A case study at Lhasa & Nyalam. *Tellus Series B, 65*, 121043. https://doi.org/10.3402/tellusb.v65i0.21043

Gonfiantini, R., Roche, M., Olivry, J., Fontes, J., & Zuppi, G. M. (2001). The altitude effect on the isotopic composition of tropical rains. *Chemical Geology*, *181*(1-4), 147–167. https://doi.org/10.1016/S0009-254(01)00279-0

Gröning, M., Lutz, H. O., Roller-Lutz, Z., Kralik, M., Gourcy, L., & Poltenstein, L. (2012). A simple rain collector preventing water re-evaporation dedicated for $\delta^{18}O$ and $\delta^2H$ analysis of cumulative precipitation samples. *Journal of Hydrology*, *448-449*, 195–200. https://doi.org/10.1016/j.jhydrol.2012.04.041

He, S., Goodkin, N. F., Ding, Q. H., Wang, X. F., Rubin, C. M., & Watts, S. (2014). Stable isotopes of daily precipitation in Singapore (2013/2014): A reflection of moisture source and atmospheric circulation, AGU Fall Meeting 2014.

He, S., Goodkin, N. F., Ding, Q. H., Wang, X. F., Rubin, C. M., & Watts, S. (2015). Stable isotopes of daily precipitation in Singapore: A preliminary study. Book of extended synopses, international symposium on isotope hydrology: Revisiting foundations and exploring Frontiers, Vol. 3: 56-59.

Houze, R. A. Jr. (1997). Stratiform precipitation in regions of convection: A meteorological paradox? *Bulletin of the American Meteorological Society*, *78*, 2179–2196. https://doi.org/10.1175/1520-0477(1997)078<2179:SPIROC>2.0.CO;2

Houze, R. A. Jr. (2004). Mesocale convective systems. *Reviews of Geophysics*, *42*, RG4003. https://doi.org/10.1029/2004RG000150

Jouzel, J. (2003). Water stable isotopes: Atmospheric composition and applications in polar ice core studies. In *Treatise Geochem., 4*, (pp. 213–243). https://doi.org/10.1016/B0-08-043751-6/04040-8

Kane, R. P. (1997). Relationship of El Niño-Southern Oscillation and Pacific sea surface temperature with rainfall in various regions of the globe. *Monthly Weather Review*, *125*(8), 1792–1800. https://doi.org/10.1175/1520-0493(1997)125%3C1792:ROENOS%3E2.0.CO;2

Kurita, N. (2013). Water isotopic variability in response to mesoscale convective system over the tropical ocean. *Journal of Geophysical Research – Atmospheres*, *118*(18), 10,376–10,390. https://doi.org/10.1002/jgrd.50754

Kurita, N., Ichiyanagi, K., Matsumoto, J., Yamanaka, M. D., & Ohata, T. (2009). The relationship between the isotopic content of precipitation and the precipitation amount in tropical regions. *Journal of Geochemical Exploration*, *102*(3), 113–122. https://doi.org/10.1016/j.gexplo.2009.03.002

Kurita, N., Noone, D., Risi, C., Schmidt, G. A., Yamada, H., & Yoneyama, K. (2011). Intraseasonal isotopic variation associated with the Madden-Julian Oscillation. *Journal of Geophysical Research*, *116*, D24101. https://doi.org/10.1029/2010JD015209

Lee, J. E., & Fung, I. (2008). "Amount effect" of water isotopes and quantitative analysis of post-condensation processes. *Hydrological Processes*, *22*(1), 1–8. https://doi.org/10.1002/hyp.6637

LeGrande, A. N., & Schmidt, G. A. (2006). Global gridded data set of the oxygen isotopic composition in seawater. *Geophysical Research Letters*, *33*(12), L12604. https://doi.org/10.1029/2006GL026011

Lekshmy, P. R., Midhun, M., Ramesh, R., & Jani, R. A. (2014). $^{18}O$ depletion in monsoon rain relates to large scale organized convection rather than the amount of rainfall. *Scientific Reports*, *4*, 5661. https://doi.org/10.1038/srep05661

Li, X., & Ting, M. (2015). Recent and future changes in the Asian monsoon-Enso relationship: Natural or forced? *Geophysical Research Letters*, *42*(9), 3502–3512. https://doi.org/10.1002/2015GL063557

Lo, J. C. F., & Orton, T. (2016). The general features of tropical Sumatra squalls. *Weather*, *71*(7), 175–178. https://doi.org/10.1002/wea/2748
Madden, R. A., & Julian, P. R. (1972). Description of global-scale circulation cells in the tropics with a 40-50 day period. *Journal of the Atmospheric Sciences*, *29*(6), 1109–1123. https://doi.org/10.1175/1520-0469(1972)029%3C1109:DOGSCC%3E2.0.CO;2
Majoube, M. (1971). Fractionnement en oxygène 18 et en deutérium entre l'eau et sa vapeur. *Journal de Chimie Physique*, *68*, 1423–1436. https://doi.org/10.1051/jcp/1971681423
Masunaga, H., & Kummerow, C. D. (2006). Observations of tropical precipitating clouds ranging from shallow to deep convective systems. *Geophysical Research Letters*, *33*(16), L16805. https://doi.org/10.1029/2006GL026547
Masunaga, H., L'Ecuyer, T., & Kummerow, C. D. (2005). Variability in the characteristics of precipitation systems in the tropical Pacific. Part I: Spatial structure. *Journal of Climate*, *18*, 823–840. https://doi.org/10.1175/JCL13698.1
Moerman, J. W., Cobb, K. M., Adkins, J. F., Sodemann, H., Clark, B., & Tuen, A. A. (2013). Diurnal to interannual rainfall $\delta^{18}O$ variations in northern Borneo driven by regional hydrology. *Earth and Planetary Science Letters*, *369-370*, 108–119. https://doi.org/10.1016/j.epsl.2013.03.014
Muller, C. L., Baker, A., Fairchild, I. J., Kidd, C., & Boomer, I. (2015). Intra-event trends in stable isotopes: Exploring midlatitude precipitation using a vertically pointing micro rain radar. *Journal of Hydrometeorology*, *16*(1), 194–213. https://doi.org/10.1175/JHM-D-14-0038.1
Munksgaard, N. C., Wurster, C. M., Bass, A., & Bird, M. I. (2012). Extreme short-term stable isotope variability revealed by continuous rainwater analysis. *Hydrological Processes*, *26*(23), 3630–3634. https://doi.org/10.1002/hyp.9505
Munksgaard, N. C., Wurster, C. M., & Bird, M. I. (2011). Continuous analysis of $\delta^{18}O$ and $\delta D$ values of water by diffusion sampling cavity ring-down spectrometry: A novel sampling device for unattended field monitoring of precipitation, ground and surface waters. *Rapid Communications in Mass Spectrometry*, *25*(24), 3706–3712. https://doi.org/10.1002/rcm.5282
Permana, D. S., Thompson, L. G., & Setyadi, G. (2016). Tropical West Pacific moisture dynamics and climate controls on rainfall isotopic ratios in southern Papua, Indonesia. *Journal of Geophysical Research: Atmospheres*, *121*(5), 2222–2245. https://doi.org/10.1002/2015JD023893
Rao, N. T., Radhakrishna, B., Srivastava, R., Satyanarayana, M. T., Rao, N. D., & Ramesh, R. (2008). Inferring microphysical processes occurring in mesoscale convective systems from radar measurements and isotopic analysis. *Geophysical Research Letters*, *35*, L09813. https://doi.org/10.1029/2008GL033495
Risi, C., Bony, S., & Vimeux, F. (2008). Influence of convective processes on the isotopic composition ($\delta^{18}O$ and $\delta D$) of precipitation and water vapor in the tropics: 2. Physical interpretation of the amount effect. *Journal of Geophysical Research*, *113*, D19306. https://doi.org/10.1029/2008JD009943
Risi, C., Bony, S., Vimeux, F., Chong, M., & Descroix, L. (2010). Evolution of the stable water isotopic composition of the rain sampled along Sahelian squall lines. *Quarterly Journal of the Royal Meteorological Society*, *136*(S1), 227–242. https://doi.org/10.1002/qj.485
Risi, C., Bony, S., Vimeux, F., Descroix, L., Ibrahim, B., Lebreton, E., et al. (2008). What controls the isotopic composition of the African monsoon precipitation? Insights from event-based precipitation collected during the 2006 AMMA field campaign. *Geophysical Research Letters*, *35*, L24808. https://doi.org/10.1029/2008GL035920
Rozanski, K., Araguacuteas-Araguás, L., & Gonfiantini, R. (1993). Isotopic patterns in modern global precipitation. In P. Swart, K. C. Lohmann, & J. McKenizie (Eds.), *Climate change in continental isotopic records, Geophysical Monograph Series* (Vol. 78, pp. 1–36). Washington, DC: American Geophysical Union.
Sánchez-Murillo, R., Birkel, C., Welsh, K., Esquivel-Hernández, G., & Corrales-Salazar, J. (2016). Key drivers controlling stable isotope variations in daily precipitation of Costa Rica: Caribbean Sea versus eastern Pacific Ocean moisture sources. *Quaternary Science Reviews*, *131*, 250–261. https://doi.org/10.1016/j.quascirev.2015.08.028
Schumacher, C., & Houze, R. A. Jr. (2003). Stratiform rain in the tropics as seen by the TRMM precipitation radar. *Journal of Climate*, *16*(11), 1739–1756. https://doi.org/10.1175/1520-0442(2003)016%3C1739:SRITTA%3E2.0.CO;2
Tang, Y. M., & Yu, B. (2008). An analysis of nonlinear relationship between the MJO and ENSO. *Journal of the Meteorological Society of Japan*, *86*(6), 867–881. https://doi.org/10.2151/jmsj.86.867
Theakstone, W. H. (2011). A seven-year study of oxygen isotopes in daily precipitation at a site close to the Arctic Circle, Tustervatn, Norway: Trajectory analysis and links with the North Atlantic Oscillation. *Atmospheric Environment*, *45*(29), 5101–5109. https://doi.org/10.1016/j.atmosenv.2011.06.034
Tremoy, G., Vimeux, F., Soumana, S., Souley, I., Risi, C., Favreau, G., & Oï, M. (2014). Clustering mesoscale convective systems with laser-based water vapor $\delta^{18}O$ monitoring in Niamey (Niger). *Journal of Geophysical Research: Atmospheres*, *119*, 5079–5103. https://doi.org/10.1002/2013/JD020968
Van Geldern, R., & Barth, J. A. C. (2012). Optimization of instrument setup and post-run corrections for oxygen and hydrogen stable isotope measurements of water by isotope ration infrared spectroscopy (IRIS). *Limnology and Oceanography: Methods*, *10*(12), 1024–1036. https://doi.org/10.4319/lom.2012.10.1024
Vimeux, F., Tremoy, G., Risi, C., & Gallaire, R. (2011). A strong control of the South American SeeSaw on the intra-seasonal variability of the isotopic composition of precipitation in the Bolivian Andes. *Earth and Planetary Science Letters*, *307*(1-2), 47–58. https://doi.org/10.1016/j.epsl.2011.04.031
Vreča, P., Brenčič, M., & Leis, A. (2007). Comparison of monthly and daily isotopic composition of precipitation in the coastal area of Slovenia. *Isotopes in Environmental and Health Studies*, *43*(4), 307–321. https://doi.org/10.1080/10256010701702739
Vuille, M., Bradley, R. S., Werner, M., Healy, R., & Keimig, F. (2003). Modeling $\delta^{18}O$ in precipitation over the tropical Americas: 1. Interannual variability and climatic controls. *Journal of Geophysical Research*, *108*(D6), 4147. https://doi.org/10.1029/2001JD002038
Yi, L., & Lim, H. (2007). Semi-idealized COAMPS simulations of Sumatra squall lines: The role of boundary forcing. In W. H. Ip & Y. T. Chen (Eds.), *Solid Earth, ocean science & atmospheric science*, *Advances in Geosciences* (Vol. 9, pp. 111–124). Singapore: World Scientific. https://doi.org/10.1142/9789812708946_0009
Yoshimura, K., Kanamitsu, M., & Detttinger, M. (2010). Regional downscaling for stable water isotopes: A case study of an atmospheric rive event. *Journal of Geophysical Research*, *115*, D18114. https://doi.org/10.1029/2010JD014032
Zwart, C., Munksgaard, N. C., Kurita, N., & Bird, M. I. (2016). Stable isotopic signature of Australian monsoon controlled by regional convection. *Quaternary Science Reviews*, *151*, 228–235. https://doi.org/10.1016/j.quascirev.2016.09.010